

Crystal structure, phase stability, and electronic structure of Ti-Al intermetallics: TiAl_3

T. Hong, T. J. Watson-Yang,* and A. J. Freeman

Department of Physics and Astronomy, Northwestern University, Evanston, Illinois 60208-3112

T. Oguchi

*National Research Institute for Metals, 2-3-12 Nakameguro, Meguro-ku, Tokyo 153, Japan
and Department of Physics and Astronomy, Northwestern University, Evanston, Illinois 60208-3112*

Jian-hua Xu

*Shanghai Institute of Metallurgy, Academia Sinica, Shanghai 200050, China
and Department of Physics and Astronomy, Northwestern University, Evanston, Illinois 60208-3112*

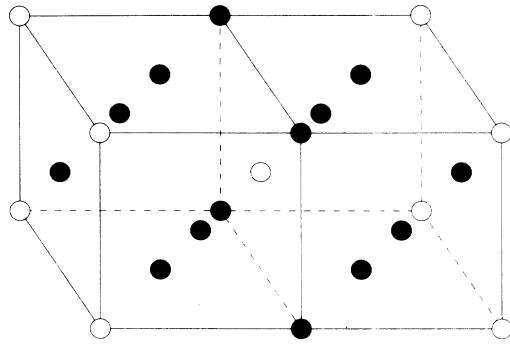
(Received 7 November 1989)

The structural phase stability and electronic properties of the intermetallic compound TiAl_3 are investigated with use of the self-consistent all-electron total-energy linear muffin-tin orbitals band-structure method within the local-density-functional approximation. The calculated equilibrium volumes have a Wigner-Seitz radius of 2.92 a.u. for the $D0_{22}$ and $D0_{19}$ structures, and 2.91 a.u. for the $L1_2$ structure, showing the expected consistency in the volume among the different structures. The calculated value also agrees with experiment for the $D0_{22}$ structure to within 2%. The calculated heats of formation are 0.42, 0.37, and 0.28 eV/atom for the $D0_{22}$, $L1_2$, and $D0_{19}$ lattices, respectively. The $D0_{22}$ structure is calculated to be the most stable phase, as observed experimentally. The calculated bulk moduli are 1.2, 1.5, and 1.1 Mbar for $D0_{22}$, $L1_2$, and $D0_{19}$, respectively. Among the three structures, the density of states at the Fermi energy, $N(E_F)$, is lowest in $D0_{22}$ and so is consistent with the inverse relation between $N(E_F)$ and stability found for other aluminum intermetallic compounds.

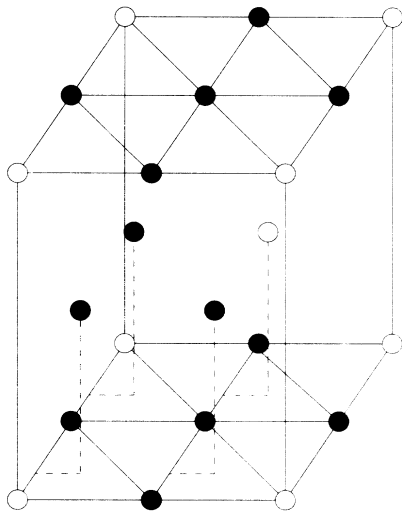
Several titanium-aluminum intermetallic compounds have a number of outstanding high-temperature properties which make them desirable candidates for high-temperature applications.¹⁻⁴ However, they have poor ductility for temperatures below a specific value (-600 – 700°C). To gain knowledge about a possible mechanism for improving the ductility, we studied the structural phase stability and electronic properties at TiAl_3 .

TiAl_3 crystallizes in the $D0_{22}$ (body-centered tetragonal) structure. The observed lattice constants are⁵ $a = 3.84 \text{ \AA}$, $c/a = 2.234$. Unlike other two titanium aluminides (Ti_3Al and TiAl),^{3,4} TiAl_3 has received little attention, though its low density ($\sim 3.3 \text{ g/cm}^3$) and high melting point (~ 1350 – 1400°C) make it especially interesting. Yamaguchi *et al.*^{6,7} have recently investigated the plastic deformation of TiAl_3 . They found that the major deformation mode is twinning of $\langle 111 \rangle \{112\}$ below 620°C . Since this structure can only provide four slip systems, then according to the von Mises criterion,⁸ the polycrystalline specimens are very brittle. At temperatures above 620°C , $[110]$ -, $[110]$ -, $[010]$ - type slips appear as augmentation of the $\langle 111 \rangle \{112\}$ slip. As a result, a good compression ductility is observed. From this result, it is very obvious that if one can find the way to ease the formation of $[110]$ -, $[100]$ -, $[010]$ -type slips at lower temperature, we might expect to obtain good ductility for this material in a wider temperature range. This paper is a first step in such a direction.⁹

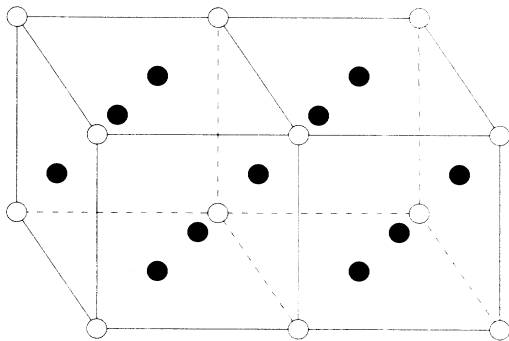
First, we studied the phase stability of TiAl_3 from a microscopic point of view. We have used the local-density linear muffin-tin orbitals (LMTO) method¹⁰ with the atomic-sphere approximation (ASA). The core electrons have been treated fully relativistically, and spin-orbit coupling has been neglected for the treatment of the valence electrons. The same radius value was taken for the Wigner-Seitz spheres of Ti and Al. For the exchange and correlation potential, we have used the expression suggested by von Barth and Hedin.¹¹ We include spherical harmonics up to $l = 2$ (d orbitals) in structuring the basis functions. As hcp-based $D0_{19}$ structure has a broad range in Ti-rich side from the phase diagram¹² and the cubic $L1_2$ structure is related to the stable $D0_{22}$ structure by displacing every (001) plane by a vector of $(\frac{1}{2}, \frac{1}{2}, 0)$, which has something to do with improvement of ductility at high temperatures, as found by Yamaguchi *et al.*, we studied the $D0_{22}$, $L1_2$, and $D0_{19}$ structures [cf. Figs. 1(a)–1(c)]. The c/a ratio was kept fixed at the experimental value ($c/a = 2.234$) for the $D0_{22}$, and at the ideal value ($c/a = 0.816$) for the $D0_{19}$ structure. The self-consistent calculations were done with the number of \mathbf{k} points within an irreducible wedge of the Brillouin zone ($N_{\mathbf{k}} = 30, 90, \text{ and } 150$). Since the calculated value of the total energy decreases with an increasing number of \mathbf{k} points in the Lehmann-taut linear tetrahedron \mathbf{k} -space integration scheme, the $N_{\mathbf{k}}^{-2/3}$ relation¹³ was used to extrapolate the total energy to the case of an infinite number of \mathbf{k} points.



(a)



(b)



(c)

FIG. 1. Crystal structures of the (a) $D0_{22}$; (b) $D0_{19}$; (c) $L1_2$.

By calculating the total energy (E_{tot}) for several different lattice constants, we can establish the relationship between E_{tot} and the Wigner-Seitz radius (see Fig. 2). Fitting this relationship by a parabola, we obtain the equilibrium lattice constant corresponding to the energy minimum. The calculated equilibrium lattice constants (in Wigner sphere radii) are 2.92 a.u. for the $D0_{22}$ and $D0_{19}$ structures, and 2.91 a.u. for $L1_2$. (Calculated values for these quantities are listed in Table I.) The consistency in the atomic volume among the different structures is truly excellent. The agreement (2% of less) between the calculated values and the experimental value (2.95 a.u.) for the $D0_{22}$ phase is also very good. This small difference in the lattice constant can be seen as a general trend resulting from the local-density approach, which usually gives a slightly smaller value compared with experiments due to neglecting temperature effects.

We obtain the heats of formation from the calculated total-energy values of the three structures and those of fcc Al and hcp Ti metals. The results are 0.42, 0.37, and 0.28 eV/atom for the $D0_{22}$, $L1_2$, and $D0_{19}$ lattices, respectively; the experimental values for the $D0_{22}$ lattice are 0.38 eV/atom (Refs. 14 and 15) and 0.37 eV/atom.^{16,17} The agreement between calculation and experiments is about 10% (cf. Table I) and again shows the overestimation due to the local-density approximation. The $D0_{22}$ structure is clearly seen as the stable phase, as expected. The total-energy difference between the $D0_{22}$ and $L1_2$ structures at the equilibrium volume is substantial, 50 meV/atom (14 mRy per formula unit), whereas the $D0_{19}$ structure has an even higher total energy, which is 90 meV/atom (24 mRy per formula unit) higher than that of the $L1_2$ lattice. These values are one order of magnitude greater than the difference between the results obtained by our finite number k point and extrapolated infinite k -point results. Thus, in this case, even a 30 k -point calculation can yield very good results for the relative phase stability. The calculated bulk moduli (by parabolic fitting) are 1.2, 1.5, and 1.1 Mbar for the $D0_{22}$, $L1_2$, and $D0_{19}$ lattices, respectively. These results (the first published theoretical values for TiAl_3 , as far as we know) are within the range of bulk moduli for intermetallics. But since their calculation involves the

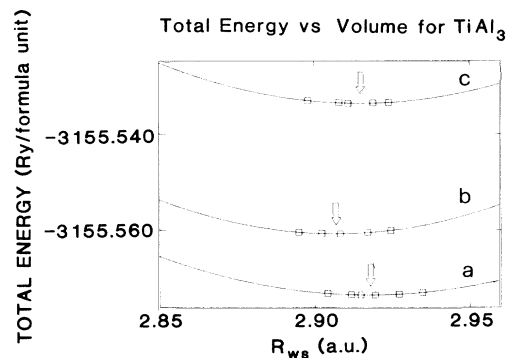
FIG. 2. Total energies vs Wigner-Seitz radius for (a) $D0_{22}$; (b) $L1_2$; (c) $D0_{19}$.

TABLE I. Comparison of calculated and experimental structural and electronic data for the three structures of TiAl_3 .

	$D0_{19}$	$L1_2$	$D0_{22}$	Expt. (for $D0_{22}$)
R_{WS} (a.u.)	2.92	2.91	2.92	2.95
ΔH (eV/atom)	0.28	0.37	0.42	0.38 (Refs. 14 and 15), 0.37 (Refs. 16 and 17)
B (Mbar)	1.1	1.5	1.2	
$N(E_F)$ (states/Ry f.u.)	40.1	25.5	24.4	
Δn^a	-1.4	-0.7	1.0	

^a Δn is the number of electrons that can be accommodated between E_F and the valley on the DOS curve. The negative values indicate the valley is lower than E_F .

second derivative of the energy, they probably have a substantial error (10–30 %).

The density-of-states (DOS) plots are given in Figs. 3–5 for the $D0_{22}$, $D0_{19}$, and $L1_2$ structures, respectively. Band compositions (by atom and orbital angular momentum) at the Γ point are listed in Table II [(a)–(c)] for the $D0_{22}$, $L1_2$, and $D0_{19}$ phases, respectively. From the Table, we can see that the compositions for the lowest Γ state are almost identical for the three phases. They are understandably dominated by the s component of the Al atoms. For $D0_{22}$, the second-lowest Γ state is a mixture of s and d from all sites, the third lowest Γ state is dominated by Al p , while the fourth (twofold degenerate) and

the fifth-lowest Γ state contain strong hybridization of Al p and Ti d , the sixth-lowest Γ state (i.e., the first unoccupied state) is dominated by Ti d . For $L1_2$, all the Γ states below the Fermi energy contain a single l component which is dominated by either Al or Ti except for the twofold-degenerate second-lowest state which is a mixture of s , and d from Al and Ti, as in the $D0_{22}$. For the $D0_{19}$, the composition of the states below the Fermi energy is more dispersive than for $D0_{22}$ and $L1_2$. They are neither as “pure” as in the $L1_2$, nor as strongly dominated by hybridization of Al p and Ti d as in the $D0_{22}$. By examining the band compositions at other points in the zone, it is observed that band characters can be essential-

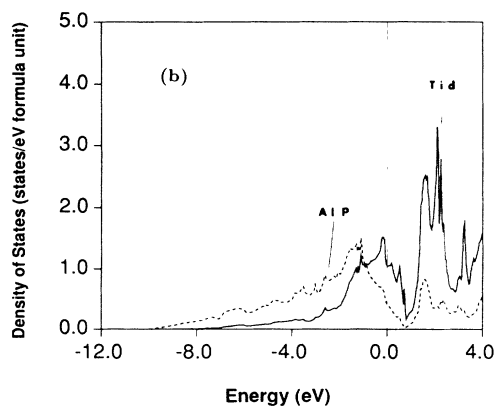
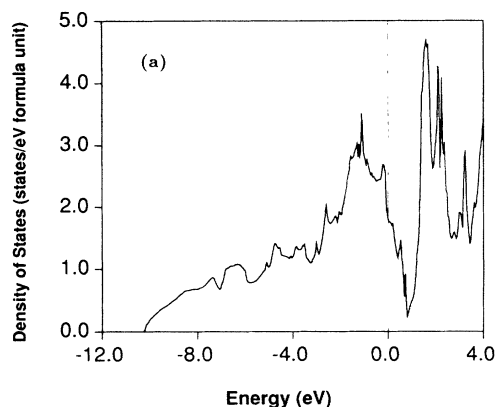


FIG. 3. Calculated (a) density of states and (b) Ti d and Al p partial density of states for TiAl_3 ($D0_{22}$).

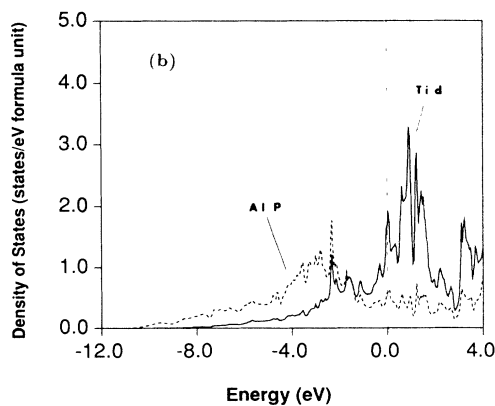
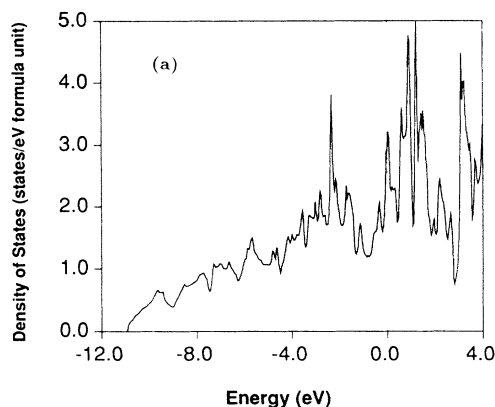


FIG. 4. Calculated (a) density of states and (b) Ti d and Al p partial density of states for TiAl_3 ($D0_{19}$).

ly represented by those at the Γ point.

Considering that the DO_{22} is calculated to be the most stable phase, we expect the hybridization between Al p and Ti d to play an important role. From the total density-of-states plots, we can see that the strongest bonding-antibonding separation appears in the DO_{22} structure: there is a very deep valley in the DOS of DO_{22} , a not so deep one in the $L1_2$ structure, and only a shallow one in the DO_{19} structure. These results show the strongest hybridization to exist in the DO_{22} structure, which also has the strongest directionality in bonding. The directional p and d bands of $TiAl_3$ play the dominant role in hybridization, which agrees with the general belief that strong directional bonding leads to brittleness (since slip systems are difficult to form in that case). On this basis, one can qualitatively understand the brittle nature of the $TiAl_3$ in the DO_{22} structure at lower temperatures.

To understand the relation of structure and stability, we first indicate the number and types of the first-, second-, and third-nearest neighbors in Table III. It is clear that all three structures have the same number of specific atoms (i.e., configuration) as first-nearest neighbors and that both $L1_2$ and DO_{19} have the same

configuration even to second-nearest neighbors. In the DO_{22} structure, there are two more other type atoms as second-nearest neighbors for atoms in the (001) planes which contain equal numbers of Ti and Al (denoted as type-1 Al or Al_1). Although the second-nearest neighbor configuration for atoms in the (001) planes containing only Al (type-2 Al or Al_2) remains the same in $L1_2$ and DO_{22} , when summed up there are still more Ti—Al bondings in the DO_{22} unit cell when second-nearest neighbors are considered. Similarly, there are more other type atoms as third-nearest neighbors in the $L1_2$ than in the DO_{19} structure. Therefore, strong Ti—Al bondings play a dominant role in the relative stability. Thus, it appears that the DO_{22} structure is the most stable phase because of more Ti—Al second-nearest-neighbor bonding, and that $L1_2$ is relatively more stable than DO_{19} because of more third-nearest-neighbor Ti—Al bonding. To be more specific, looking at the hybridizing region in energy space, it is obvious that both Ti d and Al p components are much stronger than are others in that region. Hence, the interaction between Ti d and Al p is overwhelmingly the important one.

The density of states at the Fermi energy, $N(E_F)$, is

TABLE II. Band composition at Γ point. Al_1 refers to Al atoms lying on the same (001) plane as Ti, while Al_2 refers to Al atoms lying on the (001) plane by themselves (cf. text).

Band number	Degeneracy	Energy (eV)	Ti	Al_1	Al_2
DO_{22}					
			(a)		
1	1	-10.28	s,14%	s,27%	s,59%
2	1	-3.0	s,5%;d,29%	s,26%;d,6%	s,18%;d,14%
3	1	-2.49	p,11%	p,35%	p,51%;d,2%
4	2	-1.35	d,36%	d,7%	p,57%
5	1	-1.18	d,63%	d,16%	p,21%
6	1	0.44	d,78%	d,16%	d,5%
Band number	Degeneracy	Energy (eV)	Ti	Al	
$L1_2$					
			(b)		
1	1	-11.07	s,14%	s,86%	
2	2	-3.26	d,42%	s,36%;d,22%	
3	3	-2.17	p,13%	p,87%	
4	3	-0.12	d,78%	d,22%	
Band number	Degeneracy	Energy (eV)	Ti	Al	
DO_{19}					
			(c)		
1	1	-10.94	s,15%	s,85%	
2	1	-5.73	s,1%;d,20%	s,55%;p,15%;d,10%	
3	1	-5.67	p,4%;d,11%	s,55%;p,17%;d,11%	
4	1	-5.64	p,5%;d,11%	s,59%;p,14%;d,12%	
5	1	-5.05	s,7%;d,6%	s,2%;p,83%;d,2%	
6	2	-4.41	p,18%;d,6%	s,24%;p,48%;d,4%	
7	1	-3.99	p,13%	p,86%;d,1%	
8	1	-2.54	s,26%	s,8%;p,43%;d,22%	
9	2	-1.32	d,63%	p,18%;d,20%	
10	2	-0.72	d,48%	p,46%;d,6%	
11	2	-0.46	p,3%;d,58%	s,4%;p,11%;d,24%	
12	1	0.17	s,4%;d,67%	p,1%;d,28%	

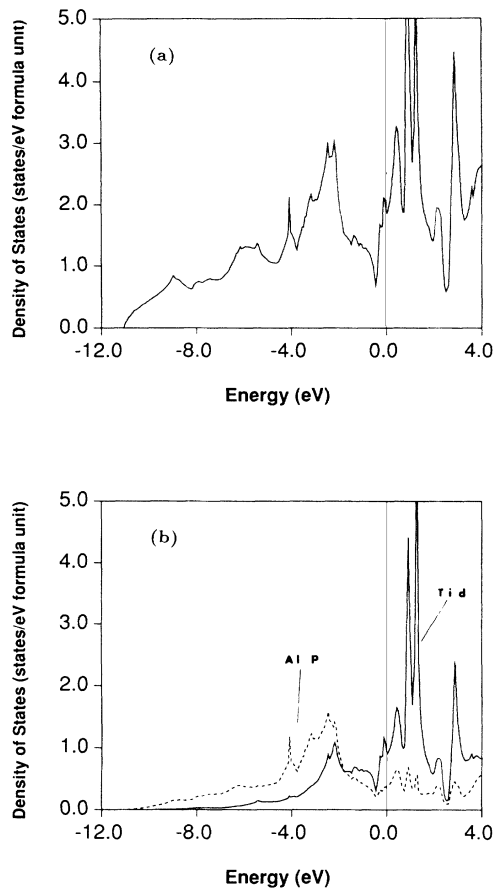


FIG. 5. Calculated (a) density of states and (b) Ti d and Al p partial density of states for TiAl_3 ($L1_2$).

TABLE III. First-nearest, second-nearest, and third-nearest-neighbor (NN) configuration for A_3B in the $L1_2$, DO_{19} , and DO_{22} structures. The atoms in the DO_{19} structure with an asterisk are actually a little closer than the rest of the third-nearest neighbors.

		First NN	Second NN	Third NN
DO_{22}	A-1	8A-2	4A-1	8A-1
		4B	2B	16A-2
		4A-1		8A-1
	A-2	4A-2	6A-2	8A-2
		4B		8B
	B	4A-1	2A-1	16A-1
$L1_2$	A	8A	6A	16A
		4B		8B
	B	12A	6B	24A
DO_{19}	A	8A	6A	12A
		4B		2A*
	B			6B
		12A	6B	18A
			2B*	

24.4, 25.5, and 40.1 states/Ry f.u. for the DO_{22} , $L1_2$, and DO_{19} structures, respectively. These values show a clear inverse relationship with stability.¹⁸ Looking at the location of the valley, which approximately separates the bonding and antibonding regions in the DOS plot, we find that the numbers of electrons, Δn , which can be accommodated below the valley energy are 1.0, -0.7 , and -1.4 valence electrons per TiAl_3 formula unit for DO_{22} , $L1_2$, and DO_{19} , respectively. Thus, as expected, accommodating more electrons in the bonding bands leads to stronger bonding.

Now, the cubic $L1_2$ phase has more slip systems than the DO_{22} and DO_{19} phases because of its higher symmetry. The $L1_2$ compounds like Cu_3Au ,¹⁹ Co_3Ti ,²⁰ and single-crystal Ni_3Al (Refs. 21 and 22) are all ductile, and even polycrystalline Ni_3Al was ductilized,²³⁻²⁵ so it is of great interest to examine our calculated results and discuss the possibility of a DO_{22} - $L1_2$ transition. To stabilize this structure, we can use rigid-band considerations as a first attempt, and add some selected lower-valence elements so that the Fermi energy of the $L1_2$ -like lattice would relocate itself in the region near the minimum in the DOS. In this case, the antibonding effect would diminish drastically. In contrast, such additions would cause E_F for the DO_{22} -like structure to climb up the peak of the DOS curve and decreased bonding would occur. As a result, the stable phase may change from DO_{22} to $L1_2$ and better ductility might possibly be obtained. However, the applicability of the rigid-band model needs to be checked out for this specific case, although it holds quite well in other studies of trialuminide systems.^{18,26} Much more computational work is needed to fully confirm this approach.

Comparing the calculated number of s , p , and d valence electrons (see Table IV) of each atom type for the three structures shows that there are more p electrons, slightly fewer d electrons, and an almost unchanged number of s electrons on the Ti site in the DO_{22} structure relative to DO_{19} and $L1_2$. The number of s electrons at the Al site is almost constant except for type-1 Al in DO_{22} . The number of p electrons at Al sites in the DO_{22} structure is a little higher at the type-2 site, and a little lower at the type-1 site than in the $L1_2$ and DO_{19} structures. The number of d electrons at the Al sites in DO_{22} is almost the same for type-1 Al and 0.03 less for type-2 Al compared to $L1_2$ and DO_{19} . These results show that the

TABLE IV. Number of electrons of different orbital angular momentum at each atom site within the muffin-tin spheres. Numbers given are meaningful only for comparisons between structures.

		s	p	d	Total
DO_{22}	Ti	0.46	0.67	2.69	3.83
	Al ₁	1.12	1.54	0.39	3.05
	Al ₂	1.06	1.60	0.39	3.06
$L1_2$	Ti	0.45	0.61	2.75	3.80
	Al	1.06	1.63	0.38	3.07
DO_{19}	Ti	0.48	0.61	2.73	3.82
	Al	1.06	1.60	0.39	3.06

effect caused by different second-nearest-neighbor configurations is substantially more significant than that caused by different third-nearest-neighbor configurations when we consider charge distribution. Different charge distribution for type-1 and type-2 Al imply stronger directionality as all the Al atoms are of same neighbor configurations in the $L1_2$ and DO_{19} structures up to second neighbors. The stronger directionality again leads to the conclusion that the formation of slip systems is more difficult in the DO_{22} structure.

In summary, we have calculated the equilibrium lattice constants, heat of formation, and bulk modulus for the DO_{22} , $L1_2$, and DO_{19} structures of $TiAl_3$. The calculated values of the first two of these physical quantities showed very good agreement with experiment for DO_{22} , while the calculated bulk moduli appear to be reasonable (in the absence of experimental data). The band structure and the

density of states clearly show stronger Ti d Al p hybridization and stronger directionality of the bonding in the DO_{22} . These factors clearly contribute to the observed absence of slip at lower temperatures in DO_{22} . From the above analysis, it appears that these first steps may point the way to obtaining improved ductility by some proper ternary additions which can affect the phase stability of the $L1_2$ phase. Clearly, more work is necessary in order to establish this direction.

ACKNOWLEDGMENTS

Work supported by the Air Force Office of Scientific Research (Grant No. 88-0346), U.S. Department of Defense and by a computing grant at the Wright-Patterson AFB Supercomputer Center. We are grateful to D. Dimiduk for discussions and encouragement.

*Present address: Department of Electrophysics, National Chiao-Tung University, 1001 Ta Hsueh Road, Hsinchu, Taiwan 30049, Republic of China.

¹*Titanium Science and Technology—Proceedings of the Fifth International Conference on Titanium*, edited by G. Lutjering, U. Zwicker, and W. Bunk (Deutsche Gesellschaft für Metallkunde e.V., Munich, 1985).

²E. W. Collings, in *The Physical Metallurgy of Titanium Alloys* (American Society for Metals, Metal Park, OH, 1984).

³H. A. Lipsitt, in *Materials Research Society Symposium Proceedings*, edited by C. C. Koch, C. T. Liu, and N. S. Stoloff (MRS, Pittsburgh, 1985), Vol. 39, p. 351.

⁴H. A. Lipsitt, in *Properties of Advanced High Temperature Alloys*, edited by S. M. Allen, R. M. Pelloux, and R. Widmer (American Society for Metals, Metal Park, OH, 1986), p. 157.

⁵W. B. Pearson, *A Handbook of Lattice Spacings and Structures of Metals and Alloys* (Pergamon, New York, 1958).

⁶M. Yamaguchi *et al.*, *Philos. Mag.* **A 55**, 301 (1987).

⁷M. Yamaguchi, Y. Umakoshi, and T. Yamane, in *Materials Research Society Symposium Proceedings*, edited by N. S. Stoloff, C. C. Koch, C. T. Liu, and O. Izumi (MRS, Pittsburgh, 1987), Vol. 81, p. 275.

⁸R. von Mises, *Z. Angew. Math. Mech.* **8**, 161 (1928).

⁹Preliminary results were presented previously, cf., T. Hong, T. J. Watson-Yang, A. J. Freeman, and T. Oguchi, *Bull. Amer. Phys. Soc.* **32**, 413 (1987).

¹⁰O. K. Anderson, *Phys. Rev. B* **12**, 3060 (1975).

¹¹U. von Barth and L. Hedin, *J. Phys. C* **5**, 1629 (1972).

¹²*Binary Alloy Phase Diagrams*, edited by T. B. Massalski (American Society for Metals, Metal Park, OH, 1986).

¹³H. J. F. Jansen and A. J. Freeman, *Phys. Rev. B* **30**, 561 (1984).

¹⁴*Selected Values of Thermodynamic Properties of Binary Alloys*, edited by R. Hultgren *et al.* (American Society for Metals, Metal Park, OH, 1973).

¹⁵O. Kubaschewski and W. A. Dench, *Acta Metall.* **3**, 339 (1955).

¹⁶*Smithells Metals Reference Book*, edited by E. A. Brandes (Butterworths, London, 1983).

¹⁷O. Kubaschewski and G. Heymer, *Trans. Faraday Soc.* **56**, 473 (1960).

¹⁸J. H. Xu, T. Oguchi, and A. J. Freeman, *Phys. Rev. B* **36**, 4186 (1987).

¹⁹B. H. Kear and H. G. Wilsdorf, *Trans. Metall. Soc. AIME* **224**, 382 (1962).

²⁰T. Takasugi and O. Ozumi, *Acta Metall.* **33**, 39 (1985).

²¹R. A. Mulford and D. P. Pope, *Acta Metall.* **21**, 1375 (1973).

²²K. Aoki and O. Izumi, *Acta Metall.* **26**, 1257 (1978).

²³K. Aoki and O. Izumi, *J. Jpn. Inst. Met.* **43**, 1190 (1979).

²⁴C. T. Liu, C. L. White, and J. A. Horton, *Acta Metall.* **33**, 213 (1985).

²⁵A. Taub, S. C. Huang, and K. M. Chang, *Metall. Trans. A* **15**, 339 (1984).

²⁶J. -H. Xu and A. J. Freeman, *Phys. Rev. B* **40**, 11 927 (1989).